International Journal for Innovative Engineering and Management Research
A Peer Revieved Open Access International Journal
www.ijiemr.org

COPY RIGHT

IJIEMR Transactions, online available on 27th Nov 2017. Link
:http://www.ijiemr.org/downloads.php?vol=Volume-6&issue=ISSUE-11

Title: **ANALYSIS OF VOLTAGE AND FREQUENCY CONTROL IN ISLANDED MICROGRID FED BLDC MOTOR DRIVE**

Volume 06, Issue 11, Pages: 349–363.
Paper Authors

P.PADMASRI, M.SUDHAKAR
KITS Engineering College, Ponnekal, Khammam (Dt), Telangana, India.

USE THIS BARCODE TO ACCESS YOUR ONLINE PAPER

To Secure Your Paper As Per UGC Guidelines We Are Providing A Electronic Bar Code

International Journal for Innovative Engineering and Management Research
A Peer Revieved Open Access International Journal
www.ijiemr.org

ANALYSIS OF VOLTAGE AND FREQUENCY CONTROL IN ISLANDED MICROGRID FED BLDC MOTOR DRIVE

[1]P.PADMASRI, [2]M.SUDHAKAR

[1]M-Tech Student Scholar,Department of Electrical & Electronics Engineering,KITS Engineering College, Ponnekal; Khammam (Dt), Telangana, India.

[2]Assistant Professor,Department of Electrical & Electronics Engineering,KITS Engineering College, Ponnekal; Khammam (Dt), Telangana, India.

Abstract: Micro grids being a new developing technology operate in two distinct modes of operation, namely, the utility-grid-connected mode and the autonomous (or islanded) mode. In transition from the utility-grid-connected mode to the autonomous mode, the frequency of a micro grid can be seriously affected due to unbalance between power generation and power demand and at that moment, micro-sources may respond slowly to eliminate this unbalancing situation. To solve this interruption and to operate the micro grid steadily, some rapid response storage systems, namely Energy Storage Systems (ESSs) are needed. The stability is an important topic to plan and manage the energy in the microgrids as the same as the conventional power systems. The voltage and frequency stability is one of the most important issues recently studied in microgrids. The objectives of this paper are the modelling and designing of the components and optimal controllers for the voltage and frequency control of the AC/DC microgrid under the different disturbances. Without using any controller, an increment in active and reactive power leads to frequency and voltage drop respectively. Therefore, droop controllers are essential in MGs. In this paper, a microgrid has been modeled and its voltage and frequency behavior in presence of BLDC motor drive characteristics has been analyzed.

Key Words: Energy storage system (ESS), microgrid (MG),P/Q droop, small-signal model, V/f droop, BLDC Motor.

I. INTRODUCTION

Nowadays most of electrical power is generated by the centralized power plants usually including large water turbines, fossil fuel combustion engines or nuclear reactors. Then, the generated power is transferred to the load centers through the most economic and effective way by the transmission lines. The centralized power generation has been used for several decades. However, there are defects in such systems, the reliability and power supply availability are the most important among them and also the long transmission lines make huge economic losses. Furthermore, given the fact that the infrastructure of the many power systems, has been used for a long time and their life is often the end, therefore they may not response to increasing electrical power requirements and their maintenance needs large financial budgets. As a result, the current power systems are usually operated around their full capacity. A blackout occurred in north east USA on August 2003 due to the overload made in a main transmission area, is a typical example for the above problems. Also, in many cases, from

International Journal for Innovative Engineering and Management Research
A Peer Revieved Open Access International Journal
www.ijiemr.org

an environmental perspective, the construction of a new large-scale power plant may not be the suitable option and even if construction is decided, selection and preparation of its location will be introduced as real challenges. To solve these inevitable problems of the concentrated power systems, application of distributed generation (DG) units in distribution systems can be considered as one of several practical and effective solutions. This application will lead to the emergence of smaller distribution networks, called microgids [1]. In general, a microgrid is a collection of micro sources and loads often providing both electricity and heat to the local area [2]. In a microgrid, a customary requirement is installing an energy storage system.In this paper, the focus will be on the control voltage of the microgrid and frequency control will be considered as one of the constraints on the problem. Design and modeling of controllers are done to control the loads bus voltage. Small disturbances (such as changes in power of the loads and generators) and large disturbances (such as a short circuit occurring on the network and transient state between two parallel and islanded operation modes) are considered to study the voltage stability of the proposed microgrid.

II. CONTROL OF MPS FOR AUTONOMOUS MG

As discussed above, the operation of an autonomous MG is usually more complex than grid-connected one since it cannot always have synchronous generators in a small and customized system. How to establish and maintain system frequency and voltage, i.e., the choice and control of MPS, is a problem in this situation. ESS with converter can be controlled flexibly with different output characteristics and is considered as a potential MPS for MG autonomous operation [21]. There are usually two typical methods that can be adopted to control ESS as a MPS, including V/f control and droop control. Due to good current sharing effect, this paper focuses on droop control. Traditional droop control named in this paper as VFDC is analyzed and compared with the proposed hybrid VFDC/PQDC.

a) VFDC

VFDC-based ESS mimics the characteristics of traditional synchronous machine with voltage angle and amplitude regulated according to its output active power and reactive power. The equivalent circuit of a MG with VFDC-based ESSs can be illustrated in Fig.1, where the two ESSs are equivalent as voltage sources$U_1\angle\varphi_1$ and$U_2\angle\varphi_2$, respectively.

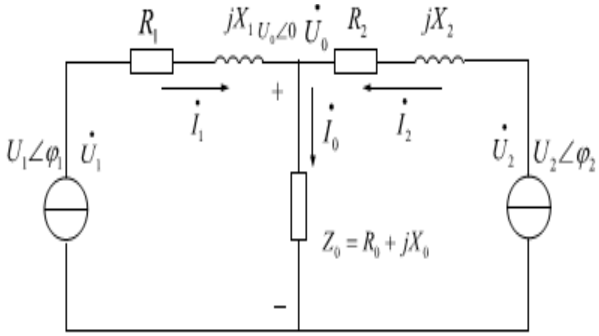

Fig.1. MG equivalent circuit based on VFDC method

The load voltage is derived from Fig.2 as

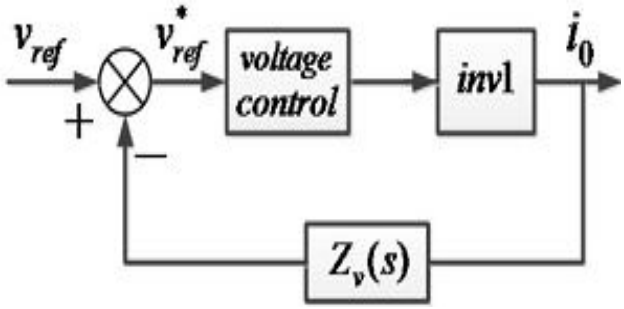

Fig.2 Schematic of virtual impedance control loop

International Journal for Innovative Engineering and Management Research
A Peer Revieved Open Access International Journal
www.ijiemr.org

$$\dot{U}_0 = \frac{\frac{\dot{U}_1}{Z_1} + \frac{\dot{U}_2}{Z_2}}{\frac{1}{Z_0} + \frac{1}{Z_1} + \frac{1}{Z_2}} \quad (1)$$

Where$Z_1 = R_1 + jX_1$ and$Z_2 = R_2 + jX_2$ are equivalent line impedance of $U_1 \angle \varphi_1$ and$U_2 \angle \varphi_2$, respectively. The outputcurrent of the two voltage sources can be derived

$$\dot{I}_1 = \frac{\dot{U}_1 - \dot{U}_0}{Z_1} = \frac{(Z_2 + Z_0)\dot{U}_1 - Z_0\dot{U}_2}{Z_1Z_2 + Z_0Z_2 + Z_1Z_0} \quad (2)$$

$$\dot{I}_2 = \frac{\dot{U}_2 - \dot{U}_0}{Z_2} = \frac{(Z_1 + Z_0)\dot{U}_2 - Z_0\dot{U}_1}{Z_1Z_2 + Z_0Z_2 + Z_1Z_0} \quad (3)$$

The apparent power of the two ESSs

$$\dot{S}_1 = \dot{U}_1 \times \dot{I}_1^* = \dot{U}_1 \times \frac{(Z_2^* + Z_0^*)\dot{U}_1^* - Z_0^*\dot{U}_2^*}{Z_1^*Z_2^* + Z_0^*Z_2^* + Z_1^*Z_0^*} \quad (4)$$

$$\dot{S}_2 = \dot{U}_2 \times \dot{I}_2^* = \dot{U}_2 \times \frac{(Z_1^* + Z_0^*)\dot{U}_2^* - Z_0^*\dot{U}_1^*}{Z_1^*Z_2^* + Z_0^*Z_2^* + Z_1^*Z_0^*} \quad (5)$$

Where the superscript * is the corresponding conjugate phasors.It can be seen from (2) to (5) that, the output current and apparent power of the two ESSs are dependent to the value of$\dot{U}_1$and$\dot{U}_2$, as well line parameters of Z_1 and Z_2.Asaresult, the current sharing of ESSs can only be implemented by the coordinated control of$\dot{U}_1$ and$\dot{U}_2$ provided that lineparametersZ_1 andZ_2 are given.

$$\frac{(Z_2 + Z_0)\dot{U}_1 - Z_0\dot{U}_2}{Z_1Z_2 + Z_0Z_2 + Z_1Z_0} = \frac{(Z_1 + Z_0)\dot{U}_2 - Z_0\dot{U}_1}{Z_1Z_2 + Z_0Z_2 + Z_1Z_0} \quad (6)$$

The phase angle difference of$\dot{U}_1$ and$\dot{U}_2$can be derived bymultiplication of$\dot{U} *_2$ to both sides of (6)

$$\angle(\varphi_2 - \varphi_1) = \frac{U_2}{U_1}\frac{2Z_0 + Z_1}{2Z_0 + Z_2} \quad (7)$$

Whereφ_1 andφ_2, U_1 andU_2 are the phase angle and voltage amplitude of$\dot{U}_1$ and$\dot{U}_2$, respectively.

$$\cos(\varphi_1 - \varphi_2) = \frac{U_2}{U_1}\frac{(2R_0 + R_1)(2R_0 + R_2) + (2X_0 + X_1)(2X_0 + X_2)}{(2R_0 + R_2)^2 + (2X_0 + X_2)^2} \quad (8)$$

$$\sin(\varphi_1 - \varphi_2) = \frac{U_2}{U_1}\frac{(2X_0 + X_1)(2R_0 + R_2) - (2R_0 + R_1)(2X_0 + X_2)}{(2R_0 + R_2)^2 + (2X_0 + X_2)^2} \quad (9)$$

From (8) and (9), it can be seen that the power distribution in the system is easily affected by line impedances. This complex the control of ESS and decreases the current sharing effect due to the uncertainty of line parameters.

b) Hybrid VFDC/PQDC

PQDC-based ESS regulates its output active power and reactive power according to MG frequency and voltage deviations from their nominal values. In Fig.1, provided that ESSU_2 is controlled with PQDC, the equivalent circuit can be described as a connection of voltage source$U_1 \angle \varphi_1$ and currentsource$I_2 \angle \varphi_2$.

According to Kirchhoff voltage and current theory, the output current of the VFDC-based voltage source$U_1 \angle \varphi_1$ is

$$\dot{I}_1 = \frac{\dot{U}_1 - \dot{I}_2 Z_0}{Z_0 + Z_1}. \quad (10)$$

Its apparent power can be derived as

$$\dot{S}_1 = \dot{U}_1 \dot{I}_1^* = \dot{U}_1 \left(\frac{\dot{U}_1 - \dot{I}_2 Z_0}{Z_0 + Z_1}\right)^* = \frac{U_1^2 - \dot{U}_1 \dot{I}_2^* Z_0^*}{Z_0^* + Z_1^*} \quad (11)$$

It can be seen that$\dot{S}_1$is independent of Z_2. If $\dot{U}_1$and line parameters are given, •S1is determined only by the value of$\dot{I}_2$. Therefore,

International Journal for Innovative Engineering and Management Research
A Peer Revieved Open Access International Journal
www.ijiemr.org

$\dot{S}_1$ and $\dot{I}_1$ can be regulated through the control of $\dot{I}_2$. As a result, the diversity and uncertainty of line parameters of Z_1 and Z_2 have no impact on MG power control. This means that the hybrid VFDC/PQDC system is better in current sharing control than the VFDC system. Though the above MG autonomous operation control scheme is ESSs-based, it is suitable for other converter based dispatch able micro resources such as single-shaft micro-turbine and fuel cell. This paper takes ESSs as example to make the analysis simple.

III. PROPOSED HYBRID VFDC/PQ DC CONTROL SCHEME

Based on the above analysis, a novel MG control method is proposed in this paper based on hybrid VFDC/PQDC. The VFDC-based ESS is controlled as a V/f droop voltage source with output voltage and frequency determined by its active power and reactive power. While the PQDC-based ESS is controlled as a P/Q source with output active power and reactive power determined by the voltage and frequency deviations on its output terminal. To decouple the active power and reactive power due to the resistive line parameters, virtual impedance control is adopted.

a) Virtual Impedance Control

According to, the active and reactive power allocation of two converters with a common bus can be expressed as

$$P = \left(\frac{EV}{Z}\cos\phi - \frac{V^2}{Z}\right)\cos\theta + \frac{EV}{Z}\sin\phi\sin\theta \quad (12)$$

$$Q = \left(\frac{EV}{Z}\cos\phi - \frac{V^2}{Z}\right)\sin\theta - \frac{EV}{Z}\sin\phi\cos\theta \quad (13)$$

Where E and V are the amplitudes of converters output voltage and bus voltage, φ is the power angle, Z and θ are the magnitude and the phase of output impedance. For high-voltage transmission system, it can be assumed that the line impedance is predominant inductive ($\theta = 90^0$). Then, (12) and (13) can be simplified as

$$P = \frac{EV}{X}\sin\phi, \quad Q = \frac{EV\cos\phi - V^2}{X} \quad (14)$$

Where X is line reactance

While for low-voltage distribution system with resistive impedance ($\theta = 0^0$), (12) and (13) can be simplified as

$$P = \frac{EV\cos\phi - V^2}{R}, \quad Q = -\frac{EV}{R}\sin\phi \quad (15)$$

Where R is line resistance

As can be seen from (14) and (15), line impedance affects the rule of active and reactive power distribution between converters. Since the $P-f$ and $Q-v$ decoupling of traditional droop control is based on inductive impedance, the control of low/medium voltage MG with resistive impedance should be adjusted. Virtual impedance control is one of the potential methods, which control converter output impedance to be inductive and then the total impedance inductive. Fig.2 shows the schematic of the virtual impedance control loop, where $Z_v(s)$ is the virtual impedance equivalent as an inductor L_v. It is in fact a voltage correction, as shown in Fig.3, where v_{ref} is the reference voltage, v^*_{ref} is that after modification, i_0 the output current, and $i_0\omega L_v$ the voltage drop on virtual inductor L_v.

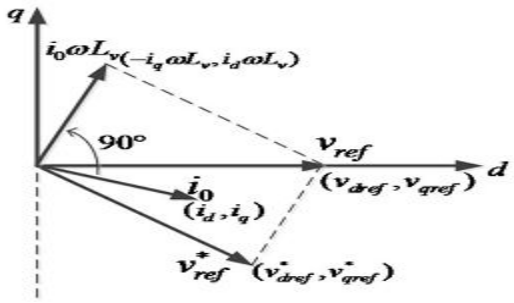

Fig.3. Phasor diagram of virtual impedance control based on d-q axis

International Journal for Innovative Engineering and Management Research
A Peer Revieved Open Access International Journal
www.ijiemr.org

The reference output voltage can be obtained

$$v_{dref}^{*} = v_{dref} + i_q \omega L_v$$
$$v_{qref}^{*} = v_{qref} - i_d \omega L_v \quad (16)$$

As a result, the equivalent impedance is controlled to be inductive which enables $P-f$ and $Q-v$ decoupling. Moreover, the active and reactive current sharing among the parallel connected ESSs can be improved since their output impedances are definite.

b) VFDC Control

The VFDC-based ESS is controlled to output certain frequency and voltage according to its active and reactive power. Since the virtual inductor L_v will absorb certain reactive powerQ_v, it is taken as a correction to the reactive power reference Q^*. The droop control loop with reactive power compensation is illustrated in Fig.4.

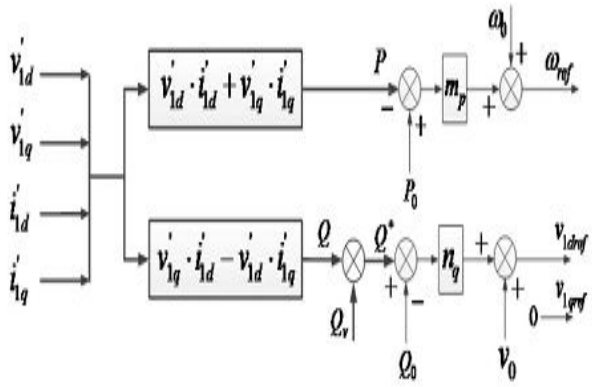

Fig.4. VFDC control loop with reactive power compensation

Therefore, the reference frequency ω_{ref} and voltage v_{ref} of VFDC converter can be written as

$$\omega_{ref} = \omega_0 + m_p \cdot (P_0 - P)$$
$$v_{ref} = v_0 + n_q \cdot (Q_0^{*} - Q) \quad (17)$$

Where P_0 and Q_0 are the rated active and reactive power, P and Q are the actual active and reactive power output, mp and n_q are the droop coefficient of active and reactive power for VFDC, w_0 and v_0 are the nominal frequency and voltage, respectively.With the reference frequency ω_{ref} and voltage v_{ref} determined, the VFDC-based converter control can be implemented with the virtual impedance loop, voltage loop, and current loop shown in Fig.5.

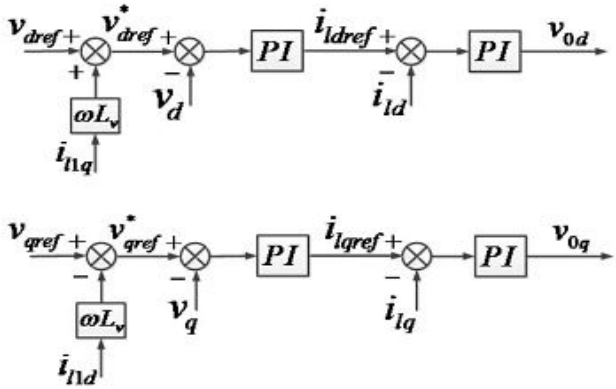

Fig.5. Virtual impedance loop, voltage loop, and current loop of VFDC ($i_{l1d}*\omega L_v$ and$i_{l1q}*\omega L_v$ denote the virtual impedance loop, respectively)

c) PQDC Control

The PQDC-based ESS is controlled to provide certain active power and reactive power according to system frequency and local voltage deviations from their nominal values.Similarly, due to the voltage drop on virtual inductor L_v, the reference voltage $v^*$is corrected with a virtual inductor voltage v_v in the droop control loop, as shown in Fig.6.

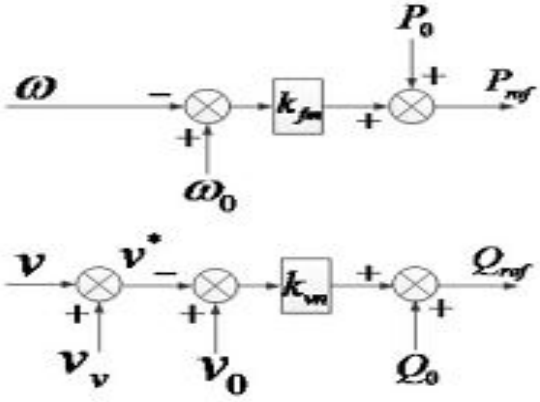

Fig.6. PQDC control loop with voltage correction

International Journal for Innovative Engineering and Management Research
A Peer Revieved Open Access International Journal
www.ijiemr.org

Therefore, the reference active and reactive power of PQ DC converter can be written as

$$P_{\text{ref}} = P_0 + k_{\text{fm}}(\omega_0 - \omega)$$
$$Q_{\text{ref}} = Q_0 + k_{\text{vn}}(v_0 - v^*) \quad (18)$$

Where k_{fm} and k_{vn} are the droop coefficient of frequency and voltage for PQDC With the reference active power P_{ref} and reactive power Q_{ref} determined, the PQDC converter control can be implemented with the virtual impedance loop, voltage loop, and current loop as shown in Figs 7 and 8, respectively.

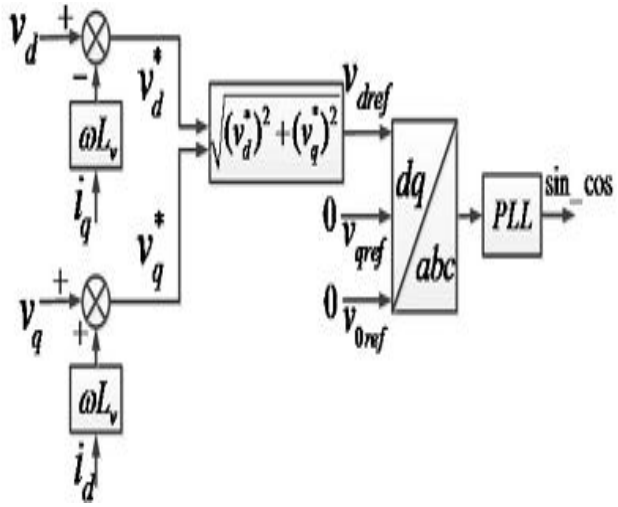

Fig.7. Virtual impedance loop of PQDC

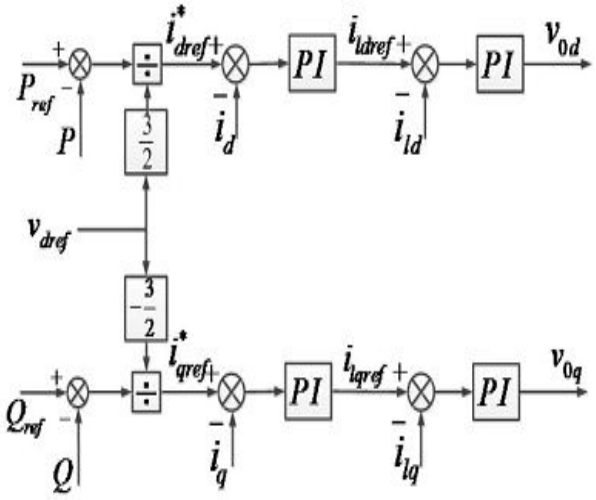

Fig.8. Voltage and current loop of PQDC

IV. SMALL-SIGNAL MODEL AND ANALYSIS

The equivalent circuit of an ESSs-based autonomous MG can be illustrated in Fig.9 The VFDC-based ESS and PQDC-based ESS connected to load (R_3, L_3, C_p) through line impedance of (R_1, L_1) and (R_2, L_2), respectively. (R_4, L_4), and (R_5, L_5) are their local loads, which can be omitted to simplify the analysis process.

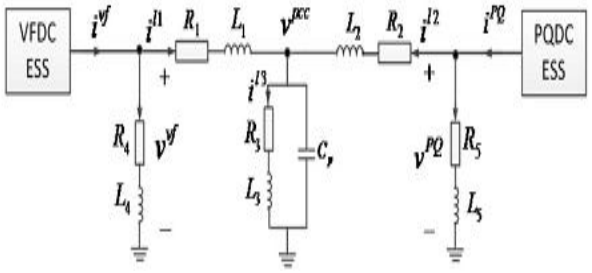

Fig.9 Equivalent circuit of ESSs-based autonomous MG

Both of the VFDC-based ESS and PQDC-based ESS is composed of a three-leg converter, LC filter, and grid coupling inductor. Fig.10 shows the diagram of ESS converter where L_{fm}, *Cfm, and* r_{fm} are filter inductor, capacitor, and equivalent resistor, respectively. L_{cm} and r_{cm} are grid coupling inductor and its equivalent resistance. The subscript denotes the type of ESS with *m=1* as the VFDC controlled ESS, *m=2*asthe PQDC one.

a) State-Space Model of VFDC-Based ESS

For VFDC-based ESS, the following equations can be derived from Fig.10:

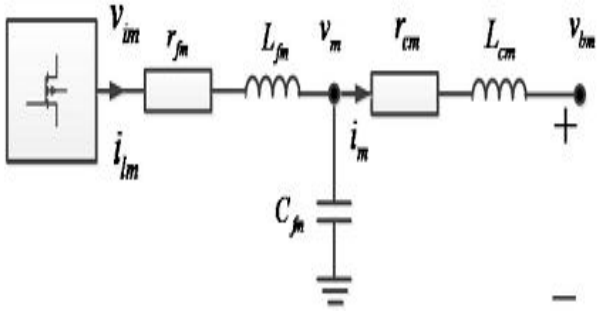

Fig.10. Equivalent circuit of the ESS converter

International Journal for Innovative Engineering and Management Research
A Peer Revieved Open Access International Journal
www.ijiemr.org

$$v_{i1} - v_1 = i_{l1} \cdot r_{f1} + L_{f1} \cdot \frac{di_{l1}}{dt}$$
$$v_1 - v_{b1} = r_{c1} i_1 + L_{c1} \cdot \frac{di_1}{dt}$$
$$C_{f1} \cdot \frac{dv_1}{dt} = i_{l1} - i_1. \quad (19)$$

The small-signal model of the power circuit of ESS in its rotary reference frame can be expressed as

$$\dot{\Delta x_1} = A_1 \Delta x_1 + B_1 \Delta v_{i1} + B_2 \Delta \omega_1 + B_3 \Delta v_{b1} \quad (20)$$
$$\Delta x_1 = \left[\Delta i_{l1d} \ \Delta i_{l1q} \ \Delta i_{1d} \ \Delta i_{1q} \ \Delta v_{1d} \ \Delta v_{1q}\right]$$
$$\Delta v_{i1} = \left[\Delta v_{i1d} \ \Delta v_{i1q}\right]$$
$$\Delta v_{b1} = \left[\Delta v_{b1d} \ \Delta v_{b1q}\right].$$

(Δi_{l1d}, Δi_{l1q}), (Δi_{1d}, Δi_{1q}), and (Δv_{1d}, Δv_{1q}) are filter inductor current, converter output current, and filter capacitor voltage in d_1-q_1 reference frame, (Δv_{i1d}, Δv_{i1q}) and(Δv_{b1d}, Δv_{b1q}) filter inductor voltage and bus voltage ind_1-q_1reference frame.ω_1 is the relative velocity of $d_1-q_1$to the global rotary reference flame.According to VFDC shown in Fig.4and (17), the increment of active power and reactive power can be derived as (21) given that v_{1dref} =v_{ref} andv_{1qref} =0

$$\Delta P = \Delta v'_{1d} \cdot i^0_{1d} + \Delta v^0_{1d} \cdot \Delta i'_{1d} + \Delta v^0_{1q} \cdot \Delta i'_{1q} + \Delta v'_{1q} \cdot i^0_{1q}$$
$$\Delta Q = \Delta v'_{1d} \cdot i^0_{1q} + v^0_{1d} \cdot \Delta i'_{1q} - v^0_{1q} \cdot \Delta i'_{1d} - \Delta v'_{1q} \cdot i^0_{1d} \quad (21)$$

Where $\Delta v'_{ld,}\Delta v'_{lq,}\Delta i'_{ld,}\Delta i'_{lq,}$are the filtered values ofΔv_{ld}, Δv_{lq}, Δi_{ld}, Δi_{lq}, v^0_{ld}, v^0_{lq}, i^0_{ld}, i^0_{lq} the steady-state value of $\Delta v'_{ld,}\Delta v'_{lq,}\Delta i'_{ld,}\Delta i'_{lq,}$ respectively.The control process of VFDC-based ESS shown inFig.3.5can be illustrated in detail in Fig.11.

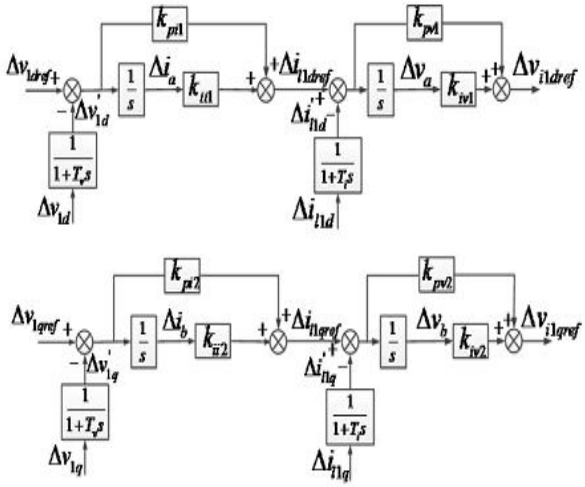

Fig.11. Voltage loop and current loop of VFDC

The filter parameters should meet the requirements

$$\frac{d\Delta i'_{l1d}}{dt} = \frac{1}{T_i}\Delta i_{l1d} - \frac{1}{T_i}\Delta i'_{l1d}$$
$$\frac{d\Delta i'_{l1q}}{dt} = \frac{1}{T_i}\Delta i_{l1q} - \frac{1}{T_i}\Delta i'_{l1q}$$
$$\frac{d\Delta v'_{1q}}{dt} = \frac{1}{T_v}\Delta v_{1q} - \frac{1}{T_v}\Delta v'_{1q}$$
$$\frac{d\Delta v'_{1d}}{dt} = \frac{1}{T_v}\Delta v_{1d} - \frac{1}{T_v}\Delta v'_{1d}$$
$$\frac{d\Delta i'_{1q}}{dt} = \frac{1}{T_i}\Delta i_{1q} - \frac{1}{T_i}\Delta i'_{1q}$$
$$\frac{d\Delta i'_{1d}}{dt} = \frac{1}{T_i}\Delta i_{1d} - \frac{1}{T_i}\Delta i'_{1d} \quad (22)$$

Where $\Delta i'_{ld}$ and $\Delta i'_{lq,}$ are the filtered values of Δi_{ld} andΔi_{lq}, respectively. Therefore, the small-signal model of VFDC based ESS can be written as

$$\dot{x}_{c1} = A_{c11}\Delta x_{c1} + A_{c12}\Delta x_1 + A_{c13}\left[\Delta v_{1\mathrm{ref}}, \Delta\omega_{1\mathrm{ref}}\right] \quad (23)$$

Where

$\Delta x_{c1} = [\Delta i'_{ld,}\Delta i'_{lq,}\Delta i'_{ld,}\Delta i'_{lq,}\Delta v'_{ld,}\Delta v'_{lq,}\Delta i_a, \ \Delta v_a, \ \Delta i_b, \ \Delta v_b, \ \Delta\omega_1]$ with Δi_a, Δv_a, Δi_b, Δv_b as control variables. Taking the reference values of Δv_{ildref} and Δv_{ilqref} being tracked, the following equation can be obtained.

$$\Delta v_{i1} = D_{11}\Delta x_{c1} + D_{12}\left[\Delta v_{1\mathrm{ref}} \quad \Delta\omega_{1\mathrm{ref}}\right] \quad (24)$$

International Journal for Innovative Engineering and Management Research
A Peer Revieved Open Access International Journal
www.ijiemr.org

Where

$$D_{11}=\begin{bmatrix} -k_{pv1} & 0 & i_{1q}^{\circ}k_{pv1}k_{pi1}n_q & -i_{1q}^{\circ}k_{pv1}k_{pi1}n_q & -k_{pi1}k_{pv1} \\ 0 & -k_{pv2} & 0 & 0 & 0 \\ -v_{1d}^{\circ}k_{pv1}k_{pi1}n_q & k_{ii1}k_{pv1} & k_{iv1} & 0 & 0 \\ -k_{pi2}k_{pv2} & 0 & 0 & k_{ii2}k_{pv2} & k_{iv2} \end{bmatrix}$$

$$D_{12}=\begin{bmatrix} k_{pv1}k_{pi1} & 0 \\ 0 & 0 \end{bmatrix}.$$

Combining (17) and (21)

$$\Delta\omega_1 = E_{11}\Delta x_{c1} + E_{12}[\Delta v_{1ref}, \Delta\omega_{1ref}] \quad (25)$$

Where

$$E_{11}=\begin{bmatrix}0 & 0 & -m_p v_{1d}^{\circ} & -m_p v_{1q}^{\circ} & -m_p i_{1d}^{\circ} & -m_p i_{1q}^{\circ} & 0 & 0 & 0 & 0\end{bmatrix}.$$

$$E_{12}=[0\ \ 1].$$

Then, (20) can be rewritten as

$$\dot{\Delta x_1} = AA_1\Delta x_1 + AB_1\Delta x_{c1} + BB_1[\Delta v_{1ref}\Delta\omega_{1ref}] + B_3\Delta v_{b1} \quad (26)$$

b) State-Space Model of PQDC-Based ESS

According to Fig.10and (19), it can be obtained

$$\Delta\dot{x_2} = A_2\Delta x_2 + B_1'\Delta v_{i2} + B_2'\Delta\omega_2 + B_3'\Delta v_{b2} \quad (27)$$

Where

$$\Delta x_2 = [\Delta i_{l2d}\ \ \Delta i_{l2q}\ \ \Delta i_{2d}\ \ \Delta i_{2q}\ \ \Delta v_{2d}\ \ \Delta v_{2q}]$$
$$\Delta v_{i2} = [\Delta v_{i2d}\ \ \Delta v_{i2q}]$$
$$\Delta v_{b2} = [\Delta v_{b2d}\ \ \Delta v_{b2q}].$$

(Δi_{l2d}, Δi_{l2q}), (Δi_{2d}, Δi_{2q}), and (Δv_{2d}, Δv_{2q}) are filter inductor current, converter output current, and filter capacitor voltage in d_2-q_2 reference frame, (Δv_{i2d}, Δv_{i2q}) and (Δv_{b2d}, Δv_{b2q}) filter inductor voltage and bus voltage. $\omega_2$is the relative velocity ofd_2-$q_2$to the global d-q reference flame.

According to PQDC control shown in Fig.3.6 and (18), the increment of active power and reactive power can be derived

$$\Delta P = \Delta v_{2d}'\cdot i_{2d}^{\circ} + v_{2d}^{\circ}\cdot\Delta i_{2d}' + v_{2q}^{\circ}\cdot\Delta i_{2q}' + \Delta v_{2q}'\cdot i_{2q}^{\circ}$$
$$\Delta Q = \Delta v_{2d}'\cdot i_{2q}^{\circ} + v_{2d}^{\circ}\cdot\Delta i_{2q}' - v_{2q}^{\circ}\cdot\Delta i_{2d}' - \Delta v_{2q}'\cdot i_{2d}^{\circ} \quad (28)$$

Where $\Delta v_{2d}', \Delta v_{2q}', \Delta i_{2d}', \Delta i_{2q}'$ are the filtered values ofΔv_{2d}, Δv_{2q}, Δi_{2d}, Δi_{2q}, v_{2d}^0, v_{2q}^0, i_{2d}^0, i_{2q}^0 the steady-state values of $\Delta v_{2d}', \Delta v_{2q}', \Delta i_{2d}', \Delta i_{2q}'$, respectively.The detailed control process of VFDC-based ESS is shown in Fig.12 with phase lock loop (PLL) illustrated in Fig.13. The actual active power and reactive power can be calculated

$$P = v_{2d}'\cdot i_{2d}' + v_{2q}'\cdot i_{2q}'$$
$$Q = v_{2d}'\cdot i_{2q}' - v_{2q}'\cdot i_{2d}'. \quad (29)$$

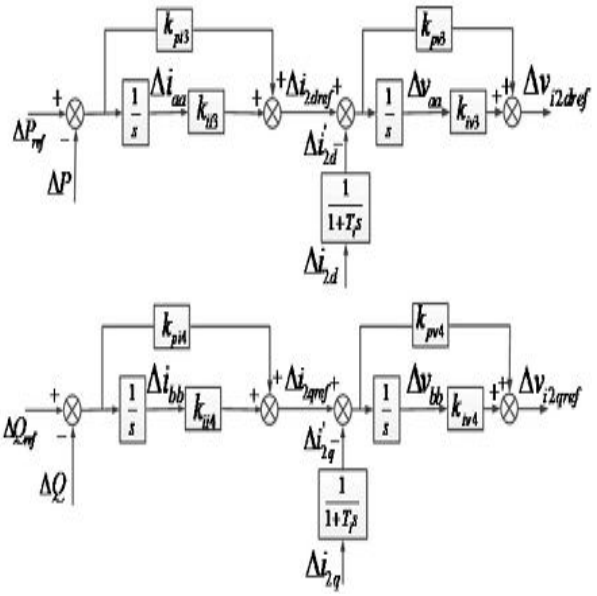

Fig.12. Voltage loop and current loop of PQDC

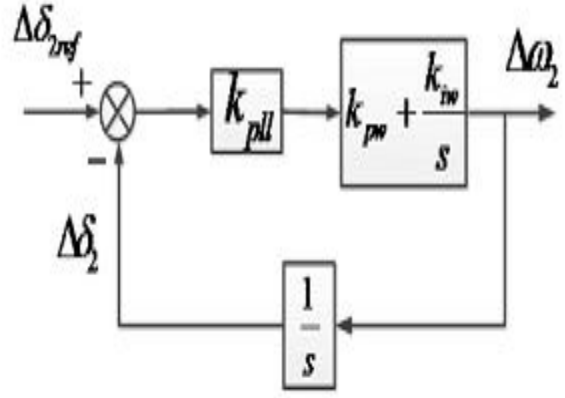

Fig.13. PLL of PQDC

International Journal for Innovative Engineering and Management Research
A Peer Revieved Open Access International Journal
www.ijiemr.org

From Fig.13, it can be derived that

$$[\Delta\delta_2] = \frac{v_{2d}^{\circ}}{(v_{2d}^{\circ})^2+(v_{2q}^{\circ})^2}\Delta v_{2q}^{'} - \frac{v_{2q}^{\circ}}{(v_{2d}^{\circ})^2+(v_{2q}^{\circ})^2}\Delta v_{2d}^{'}$$
$$= \begin{bmatrix} 0\ 0\ 0\ 0 - \frac{v_{2q}^{\circ}}{(v_{2d}^{\circ})^2+(v_{2q}^{\circ})^2} & \frac{v_{2d}^{\circ}}{(v_{2d}^{\circ})^2+(v_{2q}^{\circ})^2} 0\ 0\ 0\ 0\ 0 \end{bmatrix} \Delta x_{c2}. \quad (30)$$

The above voltages should meet the following requirement:

$$\Delta v = \Delta v_{2d}^{'} \cdot \frac{v_{2d}^{\circ}}{v^{\circ}} + \Delta v_{2q}^{'} \cdot \frac{v_{2q}^{\circ}}{v^{\circ}} \quad (31)$$

Where

$$v^{\circ} = \sqrt{(v_{2d}^{\circ})^2 + (v_{2q}^{\circ})^2}.$$

The filter parameters should meet the requirements

$$\begin{aligned} \frac{d\Delta i_{l2d}^{'}}{dt} &= \frac{1}{T_i}\Delta i_{l2d} - \frac{1}{T_i}\Delta i_{l2d}^{'} \\ \frac{d\Delta i_{l2q}^{'}}{dt} &= \frac{1}{T_i}\Delta i_{l2q} - \frac{1}{T_i}\Delta i_{l2q}^{'} \\ \frac{d\Delta v_{2q}^{'}}{dt} &= \frac{1}{T_v}\Delta v_{2q} - \frac{1}{T_v}\Delta v_{2q}^{'} \\ \frac{d\Delta v_{2d}^{'}}{dt} &= \frac{1}{T_v}\Delta v_{2d} - \frac{1}{T_v}\Delta v_{2d}^{'} \\ \frac{d\Delta i_{2q}^{'}}{dt} &= \frac{1}{T_i}\Delta i_{2q} - \frac{1}{T_i}\Delta i_{2q}^{'} \\ \frac{d\Delta i_{2d}^{'}}{dt} &= \frac{1}{T_i}\Delta i_{2d} - \frac{1}{T_i}\Delta i_{2d}^{'} \end{aligned} \quad (32)$$

Where $\Delta i_{l2d}^{'}$ and $\Delta i_{l2q}^{'}$ are the filtered value of Δi_{l2d} and Δi_{l2q} respectively. Combining the above equation, we can get

$$\dot{x}_{c2} = A_{c21}\Delta x_{c2} + A_{c22}\Delta x_2 + A_{c23}[\Delta v_{2\text{ref}} \quad \Delta\omega_{2\text{ref}}] \quad (33)$$

Where

$\Delta x_{c2} = [\Delta i_{l2d}^{'}, \Delta i_{l2q}^{'}, \Delta i_{2d}^{'}, \Delta i_{2q}^{'}, \Delta v_{2d}^{'}, \Delta v_{2q}^{'}, \Delta i_{aa}, \Delta v_{aa}, \Delta i_{bb}, \Delta v_{bb}, \Delta\omega_2]$ with Δi_{aa}, Δv_{aa}, Δi_{bb}, Δv_{bb} as control variables. Assuming the reference values of Δv_{i2dref} and Δv_{i2qref} are tracked, (34) can be obtained.

$$\Delta v_{i2} = D_{21}\Delta x_{c2} + D_{22}[\Delta v_{2\text{ref}} \quad \Delta\omega_{2\text{ref}}] \quad (34)$$

Where

$$D_{21} = \begin{bmatrix} 0\ 0 & -k_{p3}k_{pv3}i_{2d}^{\circ} - k_{pv3} & -k_{p3}k_{pv3}i_{2q}^{\circ} & -k_{p3}k_{pv3}i_{2d}^{\circ} & -k_{p3}k_{pv3}i_{2q}^{\circ} & k_{p3}k_{pv3} & k_{iv3} & 0 & 0 & -k_{p3}k_{pv3}k_{ibn} \\ 0\ 0 & k_{pv4}k_{pv4}i_{2q}^{\circ} & -k_{pv4}k_{pv4}i_{2d}^{\circ} - k_{pv4} & -k_{pv4}k_{pv4}i_{2q}^{\circ} - k_{va}k_{pv4}k_{pv4}\frac{i_{2q}^{\circ}}{v^{\circ}} & k_{pv4}k_{pv4}i_{2d}^{\circ} - k_{va}k_{pv4}k_{pv4}\frac{i_{2d}^{\circ}}{v^{\circ}} & 0 & 0 & k_{pv4}k_{pv4} & k_{iv4} & 0 \end{bmatrix}$$
$$D_{22} = \begin{bmatrix} 0 & k_{p3}k_{pv3}k_{ibn} \\ 0 & 0 \end{bmatrix}$$

Combining Fig.13and (30)

$$\Delta\omega_2 = E_{21}\Delta x_{c2} + E_{22}[\Delta v_{2\text{ref}} \quad \Delta\omega_{2\text{ref}}] \quad (35)$$

Where

$$E_{21} = \begin{bmatrix} 0\ 0 & -\frac{1}{k_{\text{fm}}}v_{2d}^{\circ} & -\frac{1}{k_{\text{fm}}}v_{2q}^{\circ} & -\frac{1}{k_{\text{fm}}}i_{1d}^{\circ} & -\frac{1}{k_{\text{fm}}}i_{2q}^{\circ} & 0\ 0\ 0\ 0\ 0 \end{bmatrix}$$
$$E_{22} = [0\ 1].$$

Then, (27) can be rewritten as

$$\dot{\Delta x}_2 = AA_2\Delta x_2 + AB_2\Delta x_{c2} + BB_2[\Delta v_{2\text{ref}} \quad \Delta\omega_{2\text{ref}}] + B_3^{'}\Delta v_{b2} \quad (36)$$

c) Network Model

According to the equivalent MG network shown in Fig.3.9,it can be derived that

$$\begin{aligned} R_1 i^{l1} + L_1\frac{di^{l1}}{dt} &= v^{vf} - v^{pcc} \\ R_2 i^{l2} + L_2\frac{di^{l2}}{dt} &= v^{PQ} - v^{pcc} \\ R_3 i^{l3} + L_3\frac{di^{l3}}{dt} &= v^{pcc} \\ C_p\frac{dv^{pcc}}{dt} &= i^{l1} + i^{l2} - i^{l3}. \end{aligned} \quad (37)$$

It can be rewritten in matrix as

$$\dot{\Delta x}_{\text{net}} = A_{\text{net}}\Delta x_{\text{net}} + B_{\text{net}}^{vf}\Delta v^{vf} + B_{\text{net}}^{PQ}\Delta v^{PQ} \quad (38)$$

$$\Delta x_{\text{net}} = \left[\Delta i_d^{l1}\ \Delta i_q^{l1}\ \Delta i_d^{l2}\ \Delta i_q^{l2}\ \Delta i_d^{l3}\ \Delta i_q^{l3}\ \Delta v_d^{pcc}\ \Delta v_q^{pcc}\right]$$
$$\Delta v^{vf} = \left[\Delta v_d^{vf}\ \Delta v_q^{vf}\right] \quad \Delta v^{PQ} = \left[\Delta v_d^{PQ}\ \Delta v_q^{PQ}\right]$$

$(\Delta i_d^{l1}, \Delta i_q^{l1})$, $(\Delta i_d^{l2}, \Delta i_q^{l2})$, $(\Delta i_d^{l3}, \Delta i_q^{l3})$, and $(\Delta v_d^{PCC}, \Delta v_q^{PCC})$ are the *d-q* components of L_1, L_2 and L_3 current and PCC voltage in the global frame, $(v_d^{vf}, \Delta v_q^{vf})$ and $(\Delta v_d^{PQ}, \Delta v_q^{PQ})$ the voltage of VFDC- based ESS and PQDC- based ESS in the global frame, respectively.

d) Complete MG Model

Taking the reference frame of the VFDC-based ESS as the global reference of the MG system, all the other ESSs, loads, and network are transited to this global reference frame through the following transformation:

International Journal for Innovative Engineering and Management Research
A Peer Revieved Open Access International Journal
www.ijiemr.org

$$\Delta i^{PQ} = T_s \begin{bmatrix} 0 & 0 & 1 & 0 & 0 & 0 \\ 0 & 0 & 0 & 1 & 0 & 0 \end{bmatrix} \Delta x_2 + T_C [\Delta \delta_2] \quad (39)$$

Where

$$T_s = \begin{bmatrix} \cos\delta_0 & -\sin\delta_0 \\ \sin\delta_0 & \cos\delta_0 \end{bmatrix} \quad T_C = \begin{bmatrix} -I_{2d}^{\circ}\sin\delta_0 - I_{2q}^{\circ}\cos\delta_0 \\ I_{2d}^{\circ}\cos\delta_0 - I_{2q}^{\circ}\sin\delta_0 \end{bmatrix}$$

And

$$[\Delta v_{b2}] = T_s^{-1} \left[\Delta v^{PQ}\right] + T_v [\Delta \delta_2] \quad (40)$$

Where

$$T_v = \begin{bmatrix} -v_d^{PQ^{\circ}} \sin\delta_0 + v_q^{PQ^{\circ}} \cos\delta_0 \\ -v_d^{PQ^{\circ}} \cos\delta_0 - v_q^{PQ^{\circ}} \sin\delta_0 \end{bmatrix}$$

$v_d^{PQ^0}$ And$v_q^{PQ^0}$ are the steady – state value of v_d^{PQ} andv_q^{PQ}.

As to the VFDC-based ESS, the following conditions should be met in the global reference frame:

$$v^{vf} = R_4 \left(i^{vf} - i^{I1}\right) + L_4 \frac{d\left(i^{vf} - i^{I1}\right)}{dt}. \quad (41)$$

It can be rewritten as

$$\begin{aligned} \Delta v^{vf} = & \begin{bmatrix} -R_4 & L_4\omega_e \\ -L_4\omega_e & -R_4 \end{bmatrix} \begin{bmatrix} 1 & 0 & 0 & 0 & 0 & 0 & 0 & 0 \\ 0 & 1 & 0 & 0 & 0 & 0 & 0 & 0 \end{bmatrix} \Delta x_{\text{net}} \\ & + \begin{bmatrix} -L_4 & 0 \\ 0 & -L_4 \end{bmatrix} \begin{bmatrix} 1 & 0 & 0 & 0 & 0 & 0 & 0 & 0 \\ 0 & 1 & 0 & 0 & 0 & 0 & 0 & 0 \end{bmatrix} \Delta \dot{x}_{\text{net}} \\ & + \begin{bmatrix} R_4 & -L_4\omega_e \\ \omega_e L_4 & R_4 \end{bmatrix} \begin{bmatrix} 0 & 0 & 1 & 0 & 0 & 0 \\ 0 & 0 & 0 & 1 & 0 & 0 \end{bmatrix} \Delta x_1 \\ & + \begin{bmatrix} L_4 & 0 \\ 0 & L_4 \end{bmatrix} \begin{bmatrix} 0 & 0 & 1 & 0 & 0 & 0 \\ 0 & 0 & 0 & 1 & 0 & 0 \end{bmatrix} \Delta \dot{x}_1 \end{aligned} \quad (42)$$

Similarly, as to the PQDC-based ESS, the following conditions should be met in the global reference frame:

$$v^{PQ} = \frac{d\left(i^{PQ} - i^{I2}\right)}{dt} L_5 + \left(i^{PQ} - i^{I2}\right) R_5. \quad (43)$$

It can be rewritten as

$$\Delta v^{PQ} = E_{21}\Delta x_{\text{net}} + E_{22}\Delta \dot{x}_{\text{net}} + D_{21}\Delta i^{PQ} + D_{22}\Delta \dot{i}^{PQ} \quad (44)$$

Where

$$E_{21} = \begin{bmatrix} -R_5 & L_5\omega_e \\ -L_5\omega_e & -R_5 \end{bmatrix} \begin{bmatrix} 0 & 0 & 1 & 0 & 0 & 0 & 0 & 0 \\ 0 & 0 & 0 & 1 & 0 & 0 & 0 & 0 \end{bmatrix}$$

$$E_{22} = \begin{bmatrix} -L_5 & 0 \\ 0 & -L_5 \end{bmatrix} \begin{bmatrix} 0 & 0 & 1 & 0 & 0 & 0 & 0 & 0 \\ 0 & 0 & 0 & 1 & 0 & 0 & 0 & 0 \end{bmatrix}$$

$$D_{21} = \begin{bmatrix} R_5 & -L_5\omega_e \\ L_5\omega_e & R_5 \end{bmatrix}$$

$$D_{22} = \begin{bmatrix} L_5 & 0 \\ 0 & L_5 \end{bmatrix}.$$

Therefore, the MG global small-signal model can be derived

$$\begin{bmatrix} \Delta \dot{x}_1 \\ \Delta \dot{x}_{c1} \\ \Delta \dot{x}_2 \\ \Delta \dot{x}_{c2} \\ \Delta \dot{x}_{\text{net}} \end{bmatrix} = [A] \begin{bmatrix} \Delta x_1 \\ \Delta x_{c1} \\ \Delta x_2 \\ \Delta x_{c2} \\ \Delta x_{\text{net}} \end{bmatrix} + [B] \begin{bmatrix} \Delta v_{1\text{ref}} \\ \Delta \omega_{1\text{ref}} \\ \Delta v_{2\text{ref}} \\ \Delta \omega_{2\text{ref}} \end{bmatrix}. \quad (45)$$

V. BLDC MOTOR

High efficiency, high power density and wide range speed controllability of BLDC motors make them suitable in various drive applications. In particular the spindle motors used in computer hard disk drives are to possess high speed characteristics for fast data access.

Brushless Direct Current (BLDC) motors are one of the motor types rapidly gaining popularity. BLDC motors are used in industries such as Appliances, Automotive, Aerospace, Consumer, Medical, Industrial Automation equipment and Instrumentation. As the name implies, BLDC motors do not use brushes for commutation; instead, they are electronically com- mutated. BLDC motors have many advantages over brushed DC motors and induction motors. A few of these are:

- Better speed versus torque characteristics
- High dynamic response
- High efficiency
- Long operating life
- Noiseless operation
- Higher speed ranges

In addition, the ratio of torque delivered to the size of the motor is higher, making it useful in

International Journal for Innovative Engineering and Management Research
A Peer Revieved Open Access International Journal
www.ijiemr.org

applications where space and weight are critical factors. In this application note, we will discuss in detail the construction, working principle, characteristics and typical applications of BLDC motors.

A) Main Characteristics BLDC Motor

Brushless DC motors consist of two coaxial magnetic armatures separated by an air gap. In certain types of motor,

- The external armature, the stator, is fixed.
- The internal armature, the rotor, is mobile (the rotor can also be external in certain cases).
- The stator is the induced part of the machine.
- The rotor is the inductor of the machine.
- In brushless DC motors, the internal armature, the rotor, is a permanent magnet. This armature is supplied by a constant current (DC).
- The external armature (stator) is poly phased (3 phases in our case) and is covered by poly- phased currents.

In a Brushless DC motor, the rotor is a permanent magnet, this type of motor has almost the same properties and physical laws as a DC current machine.

An electric motor transforms electrical energy into mechanical energy. Two main characteristics of a brushless DC motor are:

- It has an electromotive force proportional to its speed
- The stator flux is synchronized with the permanent magnet rotor flux.

VI. MATLAB/ SIMULATION RESULTS

Case 1: PQ Control with fixed load

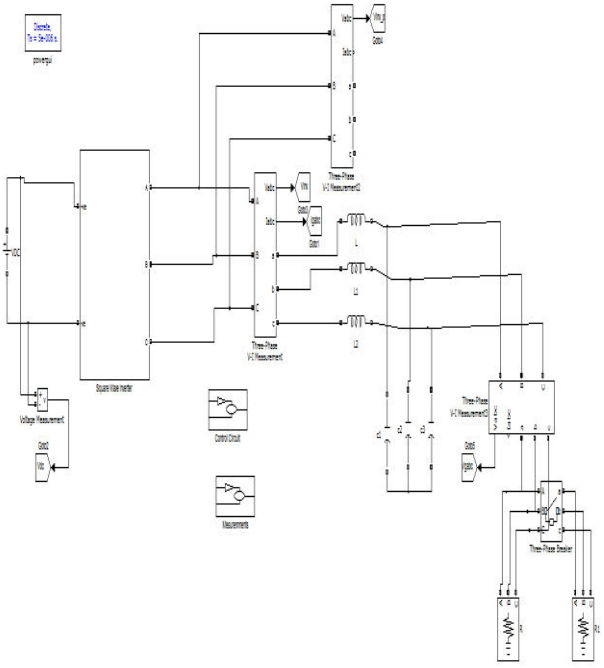

Fig.14 Matlab/Simulink model of PQ control with fixed load

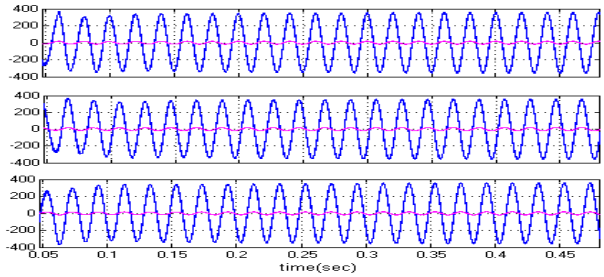

Fig.15 Steady-state voltage and current curves

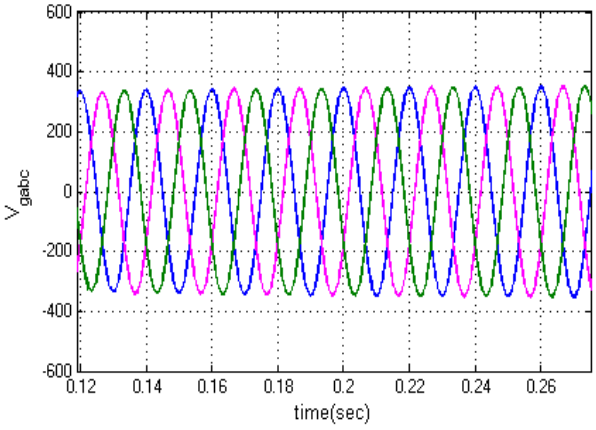

Fig.16 Source Voltages (V)

International Journal for Innovative Engineering and Management Research
A Peer Revieved Open Access International Journal
www.ijiemr.org

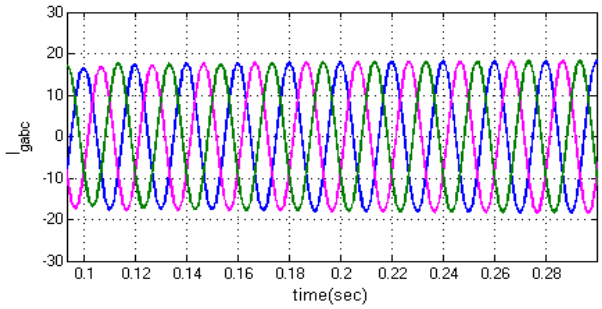

Fig.17 Source Currents (A)

Case: 2 PQ Control variable Decremental load

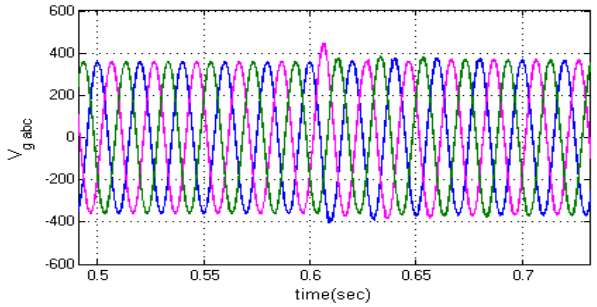

Fig.18 Source Voltages (V)

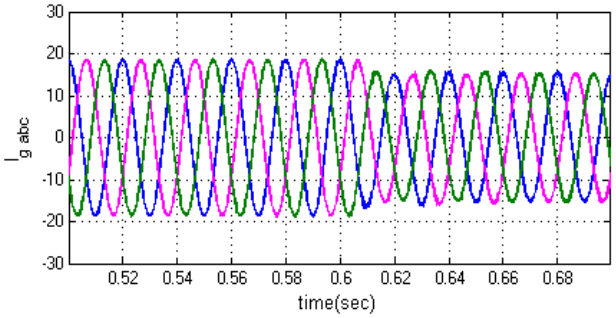

Fig.19 Source Currents (A)

Case: 3 PQ Control variable Incremental load

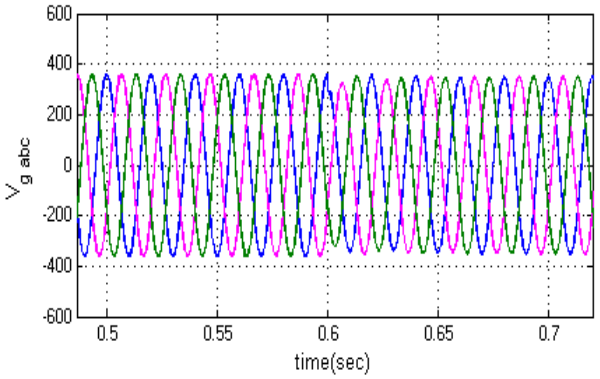

Fig.20 Source Voltages (V)

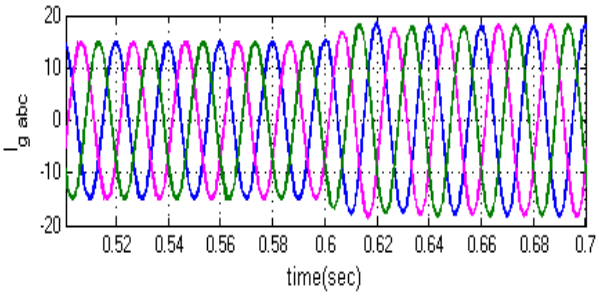

Fig.21 Source Currents (A)

Case: 4 VF control Fixed load

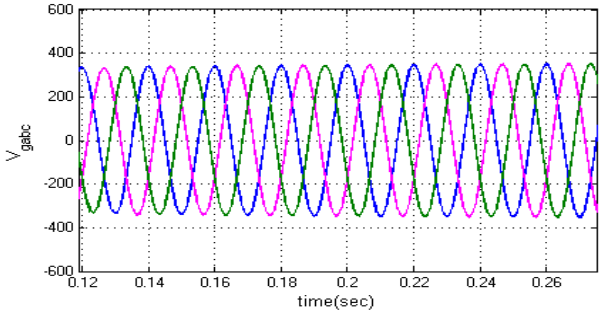

Fig.22 Source Voltages (V)

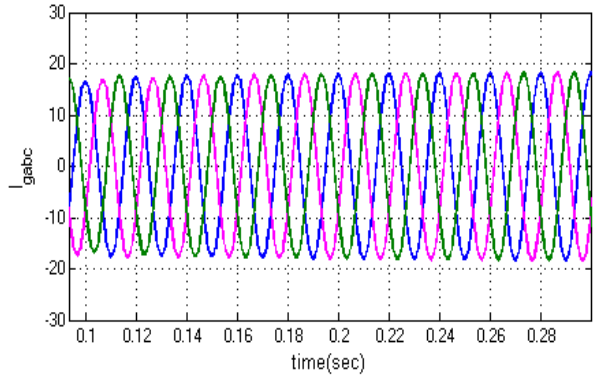

Fig.23 Source Currents (A)

Case: 5 VF control variable with Decremental load

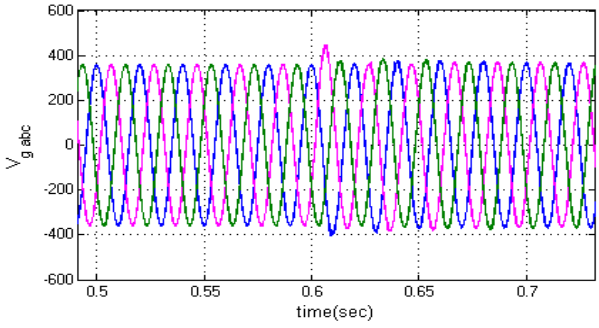

Fig.24 Source Voltages (V)

International Journal for Innovative Engineering and Management Research
A Peer Revieved Open Access International Journal
www.ijiemr.org

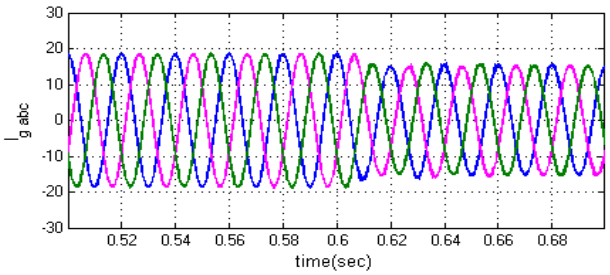

Fig.25 Source Currents (A)

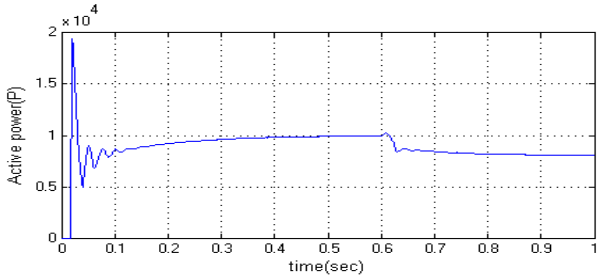

Fig.26 Active Power (P)

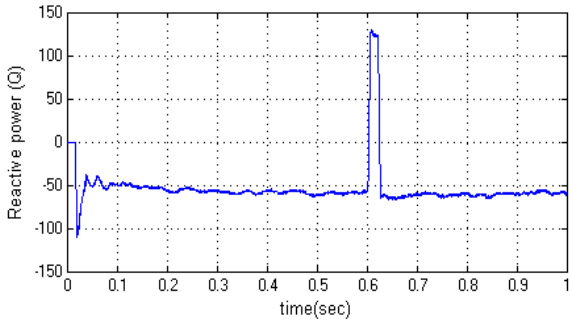

Fig.27 Reactive Power (Q)

Case: 6 VF control variable with Incremental load

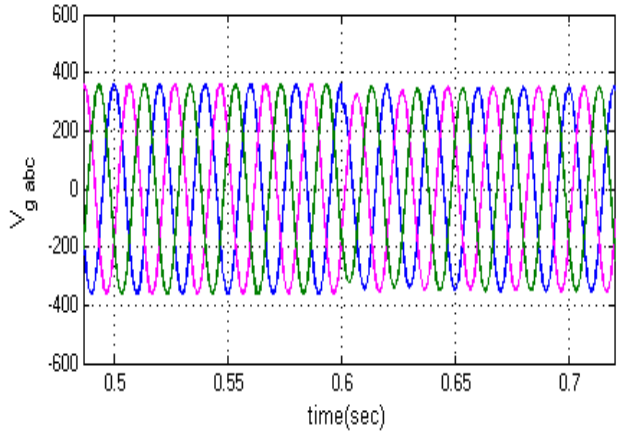

Fig.28 Source Voltages (V)

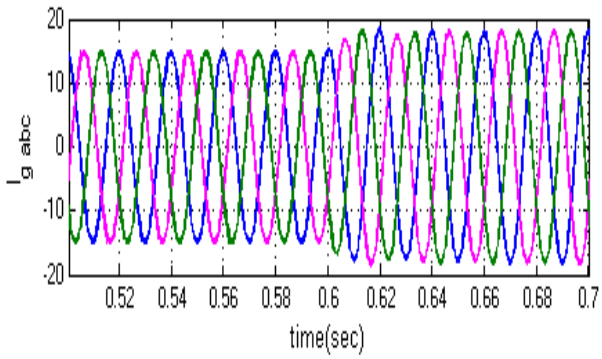

Fig.29 Source Currents (A)

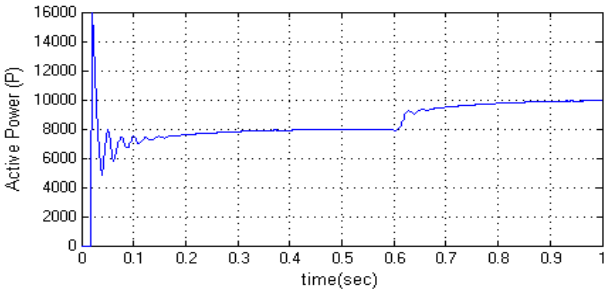

Fig.30 Active Power (P)

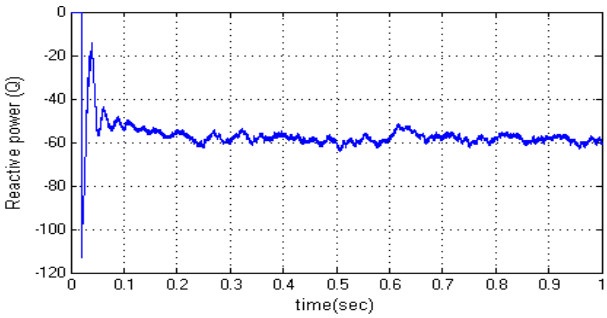

Fig.31 Reactive Power (Q)

Case: 7 PQ control fixed load with BLDC Motor

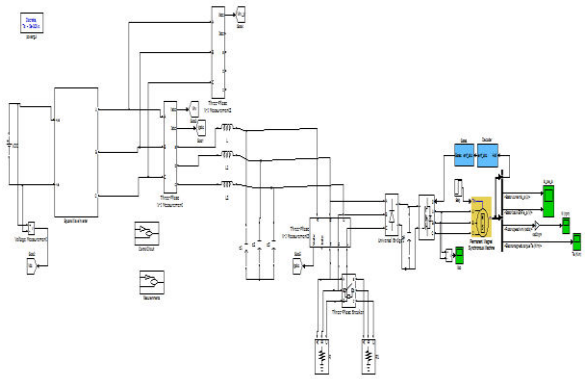

Fig.32 Matlab/Simulink model of BLDC motor with fixed load

International Journal for Innovative Engineering and Management Research
A Peer Revieved Open Access International Journal
www.ijiemr.org

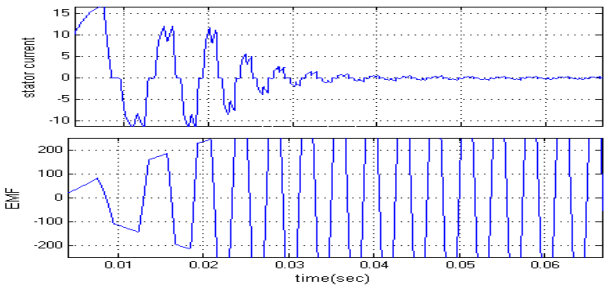

Fig.33 Stator Current (A) and EMF of the BLDC motor

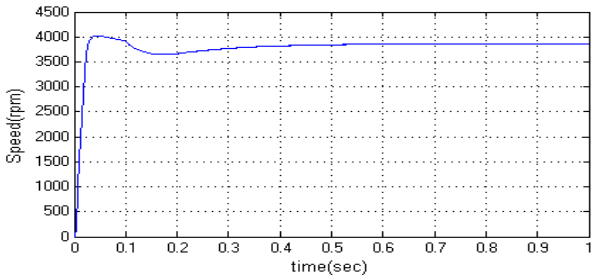

Fig.34 Speed Curve of the BLDC motor

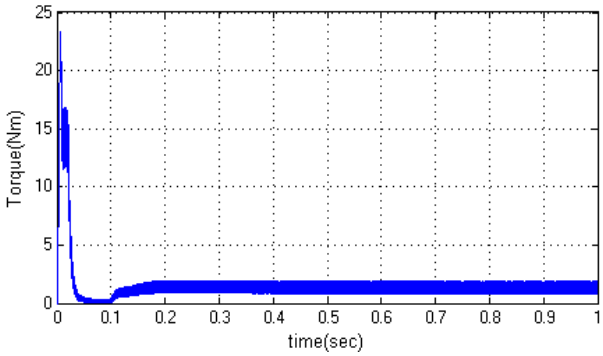

Fig.35 Torque Characteristics of the BLDC Motor

VII. CONCLUSION

In this paper proposes a voltage and frequency is controlled by energy storage system. For this purpose, a droop control strategy is used as follows. For the verification of the correct operation of the energy storage system, several different scenarios, including the disconnection of the microgrid from the main grid and the constant variation of the load in the islanding mode, are designed. Characteristics of a BLDC motor as a sample load was observed by Matlab simulation results. It was concluded that both the duration and intensity of the fault can determine how the frequencies of different DGs in the microgrid will be stabilized.

REFERENCES

[1] R. H. Lasseter, "Microgrids," in Proc. IEEE Power Eng. Soc. Winter Meeting, New York, NY, USA, Jan. 2002, pp. 305–308.

[2] A. G. Tsikalakis and N. D. Hatziargyriou, "Centralized control for optimizing microgrids operation," IEEE Trans. Energy Convers., vol. 23, no. 1, pp. 241–248, Mar. 2008.

[3] H. Nikkhajoei and R. H. Lasseter, "Distributed generation interface to the CERTS microgrid," IEEE Trans. Power Del., vol. 24, no. 3, pp. 1598–1608, Jul. 2009.

[4] X. Tang and Z. Qi, "Energy storage control in renewable energy based microgrid," in Proc. IEEE Power Energy Soc. Gen. Meeting, San Diego, CA, USA, Jul. 2012, pp. 1–6.

[5] J.Y.Kimet al., "Cooperative control strategy of energy storage system and microsources for stabilizing the microgrid during islanded operation," IEEE Trans. Power Electron., vol. 25, no. 12, pp. 3037–3048, Dec. 2010.

[6] X. Tang, W. Deng, and Z. Qi, "Investigation of the dynamic stability of microgrid," IEEE Trans. Power Syst., vol. 29, no. 2, pp. 698–706, Mar. 2014.

[7] M. C. Chandorkar, D. M. Divan, and R. Adapa, "Control of parallel connected inverters in standalone AC supply systems," IEEE Trans. Ind. Appl., vol. 29, no. 1, pp. 136–143, Jan./Feb. 1993.

[8] Y. Li and C.-N. Kao, "An accurate power control strategy for power-electronics-interfaced distributed generation units operating in a low-voltage multibus microgrid," IEEE Trans. Power Electron., vol. 24, no. 12, pp. 2977–2988, Dec. 2009.

[9] J. A. P. Lopes, C. L. Moreira, and A. G. Madureira, "Defining control strategies for microgrid islanded operation," IEEE Trans. Power Syst., vol. 21, no. 2, pp. 916–924, May 2006.
[10] J. M. Guerreroet al., "Wireless-control strategy for parallel operation of distributed-generation inverters," IEEE Trans. Ind. Appl., vol. 53, no. 5, pp. 1461–1470, Oct. 2006.
[11] J. M. Guerreroet al., "Droop control method for the parallel operation of online uninterruptible power systems using resistive output impedance," in Proc. 21st Annu. IEEE Appl. Power Electron. Conf. Expo. (APEC), Dallas, TX, USA, Mar. 2006, pp. 1716–1722.
[12] J. M. Guerrero et al., "Droop control method with virtual output impedance for parallel operation of uninterruptible power supply systems in a microgrid," in Proc. 22nd Annu. IEEE Appl. Power Electron. Conf. (APEC), Anaheim, CA, USA, Mar. 2007, pp. 1126–1132.
[13] J. He et al., "An islanding microgrid power sharing approach using enhanced virtual impedance control scheme," IEEE Trans. Power Electron., vol. 28, no. 11, pp. 5272–5282, Nov. 2013.
[14] E. Barklundet al., "Energy management in autonomous microgrid using stability-constrained droop control of inverters," IEEE Trans. Power Electron., vol. 23, no. 5, pp. 2346–2352, Sep. 2008.
[15] Y. A. I. Mohamed and E. F. El-Saadany, "Adaptive decentralized droop controller to preserve power sharing stability of paralleled inverters in distributed generation microgrids," IEEE Trans. Power Electron., vol. 23, no. 6, pp. 2806–2816, Nov. 2008.